Journal of Power Sources 629 (2025) 236019

Contents lists available at ScienceDirect

Journal of Power Sources

journal homepage: www.elsevier.com/locate/jpowsour

Stack pressure on lithium-ion pouch cells: A comparative study of constant pressure and fixed displacement devices

Adriano Schommer *, Miguel Orozco Corzo, Paul Henshall, Denise Morrey, Gordana Collier

Faculty of Technology, Design and Environment, Oxford Brookes University, Wheatley Campus, Oxford, OX33 1HX, UK

HIGHLIGHTS

- Stack pressure variation is significantly different among the fixtures tested.
- Spring-based fixtures offer a robust solution to apply stack pressure.
- Fixed displacement devices fail to mitigate cell relaxation effects.
- Pneumatic devices are best explored with active pressure control.

ARTICLE INFO

Dataset link: https://doi.org/10.5281/zenodo.13755167

Keywords:
Stack pressure
Constant pressure
Constant displacement
Pressure profile
Fixture design

ABSTRACT

This study addresses the effects of stack pressure on lithium-ion pouch cells by comparing different fixture designs and their impact on variation of stack pressure with time. While previous research has examined pouch cell performance under varying stack pressures, a comprehensive comparison of fixture types and their influence on pressure variation has been lacking. This research provides insights for researchers in selecting appropriate fixture designs for their specific investigations. Two categories of fixtures were investigated: constant pressure fixtures (utilizing springs and a passive pneumatic system) and fixed displacement fixtures (employing bolted plates). The experiments evaluated the pressure loss from an initial static pressure of 90 kPa over a 48h resting period, in addition to the pressure changes under dynamic load profiles. Our findings reveal that, under dynamic loading, the fixed displacement fixture exhibited a pressure variation five times higher than the constant pressure device using springs, and 3.7 higher than the pneumatic device. Additionally, the results demonstrated that the fixed displacement device is unable to mitigate the pressure loss due to relaxation effects of the cell and the bolted connections. In contrast, the spring-based fixture offered a simple and effective solution to hold pressure during experiments.

1. Introduction

The growing demand for electric vehicles in many countries and subsequently for lithium-ion batteries has also resulted in a significant need to improve lithium-ion cell testing and characterization to optimize cell performance and prolong battery pack lifetime. There are three different types of Li-ion cells, cylindrical, prismatic and pouch cells. Cylindrical cells have been the most commonly used over the years for electric vehicle applications [1]. However, pouch cells are currently gaining significant attention in the field because they offer a viable solution to increase packaging and power density compared to the other cell types. Despite this benefit, pouch cells also face different challenges compared to other cell types, such as swelling, high-temperature stability issues and greater vulnerability to physical damage [1]. For these reasons, pouch cells require careful assembly and management to guarantee optimal performance.

To extend the lifetime and performance of pouch cells, several key factors should be considered that influence cell degradation, these include temperature, charge and discharge rate, state of charge (SOC), and cell swelling. With pouch cells, cell swelling occurs to some degree on both charge and discharge of the cell. Cell swelling can be an irreversible effect because of the formation of solid electrolyte interphase on the anode, which leads to loss of active lithium and reduction in cell capacity [2].

Investigations have discovered that attempting to control the stack pressure of a pouch cell via mechanical compression might translate into a positive effect on performance. Stack pressures that are too low or too high can accelerate delamination and plating degradation

* Corresponding author.
E-mail address: adriano.schommer@brookes.ac.uk (A. Schommer).

https://doi.org/10.1016/j.jpowsour.2024.236019
Received 13 September 2024; Received in revised form 22 November 2024; Accepted 3 December 2024
Available online 12 December 2024

phenomena. Furthermore, high pressures can impede ion transport, which subsequently impacts performance [2]. Cannarella et al. [3] reported that maintaining a certain optimal stack pressure to Li-ion cells maximized cell cycle life, and they also demonstrated a linear relationship between increasing peak cycle stress and decreasing cell state of health (SOH). Aiello et al. [4] found that by applying pressure, the wettability of the electrode improved. And in [5], Zhang et al. concluded that a constant stack pressure can enhance ion diffusion and that pressure variation increases at higher current rates. These performance improvements are largely a result of reducing cell swelling, enhancing the interfacial surface area between the positive and negative electrodes and the separator, and reducing the ionic resistivity [6]. Such benefits ultimately help to reduce power loss during operation.

For experimental testing, stack pressure has been applied in different forms, but it can be divided into two categories, fixed displacement and constant pressure. Stack pressure changes with SOC because of the (de)lithiation of the anode during cycling, which causes the cell to expand during charge and contract during discharge. However, how the stack pressure fixture interacts with the expansion and contraction of the cell might impact the experimental results, as different fixtures will result in different pressure variation for the same initial stack pressure.

In a study by [7], considering the performance of single lithium-ion pouch cells and coupled parallel cells to simulate battery packs, pressures of a range of 0.66–1.98 MPa were applied using a constant pressure fixture. They found that the specific capacity of the cell at the lowest pressure decreased by 18.6%, and at a pressure of 1.3 MPa decreased by 12.4% in an 3C charge and discharge ageing cycle. In [8], a bespoke control rig was developed in such a way that the cell was placed between a floating and a fixed plate. The pressure was then applied via an airbag located between the floating and the fixed plate to ensure uniform pressure distribution on the cell, the airbag was connected to an air supply regulator to maintain a constant pressure. The authors concluded that applying pressure on pouch cells increases the cell lifetime but also decreases the cell capacity by 4%. Muller et al. [9] used two different experimental setups to carry out stack pressure tests, one using a constant displacement fixture that constrained the cell to a fixed thickness, leading to variations in pressure over time by adding stiff spacers around the bolts. The other test employed a constant pressure device, replacing the spacers by coild springs. Their work revealed that pouch cells under a constant pressure of 0.42 MPa exhibited the least capacity fade. Leonard et al. [6], also used two different test set-ups for experiments, one basic fixture where the pressure was applied by fastening two parallel plates (fixed displacement), and a pneumatic system where the pressure was applied by an actuator connected to an air reservoir to counteract the cell expansion and contraction. When comparing both fixtures, the pneumatic fixture presented pressure variations lower than 25%, and the fixed displacement system presented variations greater than 300%. This suggested that incorporating a more uniform pressure on pouch cells, independent of cell swelling, could improve discharge capabilities for high-performance cells. In a study by Cannarella et al. [10], the tests were conducted by constraining the cell in a fixture with an amplified load cell and aluminium plates which were held together with nuts and bolts. The nuts and bolts were secured in position and a thread locking adhesive was applied to prevent loosening, but there was a pressure decrement which was assumed to be due to stress relaxation on the cell, because of the viscoelastic nature of the materials used. Which meant the initial set pressure only lasted for a short period of time, and it was unlikely that the targeted pressure applied remained constant.

The effects of stack pressure on cells is a relatively recent research subject. The studies reviewed previously in this introduction have focused on the performance of pouch cells under different levels of stack pressure. However, to the best of the authors' knowledge, a direct comparison of different fixtures and how the pressure profile is impacted by different concepts of the fixtures is still missing in the literature. So far, the devices can be classified into constant pressure fixtures and fixed displacement fixtures. Constant pressure fixtures rely on springs and pneumatic systems, whereas fixed displacement fixtures rely on bolted top plates. This paper focuses on the impact of these devices on the dynamic pressure variation, so that researchers are better informed about the implications of different concepts, selecting a design that better suits their investigation. Two experiments are conducted to evaluate the pressure loss of these devices from an initial stack pressure, and the pressure change under a dynamic load profile.

This paper is organized as follows. The methodology is explored in Section 2, where the experimental setup is presented, and the experiments are described. The results are then presented in Section 3, and this paper is concluded in Section 4.

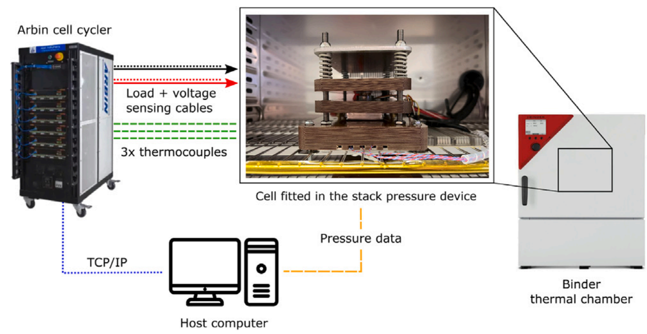

Fig. 1. Experimental setup.

2. Methodology

Two experiments were conducted using three different design concepts to apply stack pressure on a pouch cell: a fixed displacement device, a constant pressure device using coil springs, and a constant pressure device using a pneumatic actuator. Experiment I assessed the static pressure loss using a pouch cell. That is, the pressure loss due to various sources of relaxation after the cell has been calibrated to the target pressure. Experiment II evaluated the pressure loss of the devices during cycling on a Hybrid Power Pulse Characterization (HPPC) test [11].

The pressure loss is defined as in

$$\mathbf{P}_{loss} = \mathbf{P}_{1\dots n} - P_1 \mathbf{1}_n \tag{1}$$

where $\mathbf{P}$ is the vector containing the pressure measurements. The subscript indicates the data points P_1 to P_n, where P_1 is the calibration data point, and $\mathbf{1}_n$ is a vector of ones of the same dimension as $\mathbf{P}_{1\dots n}$.

2.1. Experimental setup

The experimental setup is shown in Fig. 1, and it is similar to the experimental setup employed in [6]. Two 60 A load channels of an Arbin LBT-21084-HC cell cycler were used in parallel to perform the tests. The voltage measurement precision of the cycler is rated as ±0.75 mV. The ambient temperature was controlled by a thermal chamber Binder KB115, in which the temperature fluctuation is expected to be within ±0.1 °C. Additionally, three type-T thermocouples rated to an accuracy of ±0.5 °C were used to measure the cell surface temperature at the centre, and near the negative and positive terminals.

To maintain consistent stack pressure on a pouch cell during testing, a fixture that can sustain a constant pressure is essential. Variations in pressure can confound the results, making it challenging to isolate the primary effects under investigation. To address this issue, three different fixture designs were evaluated. Fig. 2 illustrate the devices.

The fixed displacement fixture as described in [12] was developed and was the first device tested (Fig. 2a). Four threaded rods were used to compress the cell against two plates made of Tufnol, a synthetic

Table 1
Cell specifications.

Parameter	Specification
Cell	Melasta SLPBB142124
Cathode material	Lithium Cobalt Oxide (LiCoO2)
Anode material	Graphite
Form factor	Pouch
Dimensions	42 × 125 × 10.7 mm (W × H × T)
Weight	124 g
Nominal Capacity	6.8 Ah
Maximum continuous charge	2C
Maximum continuous discharge	15C
Voltage operating range	3 V–4.2 V
Operating temperature	−20–60 °C

resin, bonded and laminated composite material with high mechanical and electrical insulation properties. In an attempt to reduce the stress relaxation of the bolted connections, M4 threaded rods originally designed in [12] were substituted for M6 rods [13,14]. In addition, lock nuts were used instead of plain nuts to mitigate the risk of the torque loosening during the tests. The pressure data was computed using measurements from two TE FX29 force sensors connected to a Teensy microcontroller [6]. The location of the force sensors is demonstrated Fig. 2(d). The calibration of the stack pressure was performed using a star torque pattern, carefully torquing the nuts until a uniform force reading was achieved in both sensors for the target pressure. Fig. 2(a) also provides a detail view of the load sensor. The point of contact of the sensor is spherical, which mitigates small errors of parallelism between the two Tufnol plates. Finally, the load sensor was not applied directly to the Tufnol plate, but on a steel insert to improve the load distribution in the plate.

The constant pressure fixture using springs is illustrated in Fig. 2(b). The device was developed based on previous work of [9,12]. The main difference compared to the first device is the use of springs to compensate for the initial stress relaxation of the cell [10] and bolted connections. The underlying principle is that the cell strain after the initial preload is small enough for the spring to compensate without significantly impacting the initial stack pressure. The device uses four coil springs with a linear stiffness of 17.5 N/mm (70 N/mm in total), compressing 6.75 mm for a 90 kPa stack pressure. Considering the volumetric expansion of graphite anode to be $\approx 10\%$ and the LCO cathode to be $\approx 2\%$ [15], the theoretical volumetric expansion is expected to be in the order of 0.5 mm, which makes the spring displacement on preload one order of magnitude larger than the volumetric expansion of the cell, and the strain expected due to the stress relaxation [16].

The constant pressure fixture using a pneumatic actuator is illustrated in Fig. 2(c). The device was developed by a previous study at Oxford Brookes University [6]. The system uses a pneumatic actuator (Festo ADN-40-20-I-P-A) connected to an 2 litre air reservoir (Festo CRVZS-2) with the aim of compensating for the thickness variation of the cell at different SOCs. Instead of Tufnol plates, the device uses a carbon-reinforced 3D-printed plates. The device also features a spherical ball joint to provide rotational freedom of the compressing plate. This design ensures uniform contact between the cell and the pressure plates, making the system less sensitive to cell swelling [6].

2.2. Cell specifications

Experiments I and II were conducted on a fresh Melasta 6.8Ah lithium cobalt oxide (LCO) cell. The cell specifications are given in Table 1.

2.3. Experiment I - Static pressure loss

Experiment I tested the three devices for static pressure loss. That is, the pressure loss of the device while clamping a cell at rest (no current load applied). Each fixture was calibrated to a target pressure of 90 ± 2 kPa and then subjected to a 48-h rest period at 25 °C in a thermal chamber. The pressure target was chosen to be consistent with previous tests performed in [6].

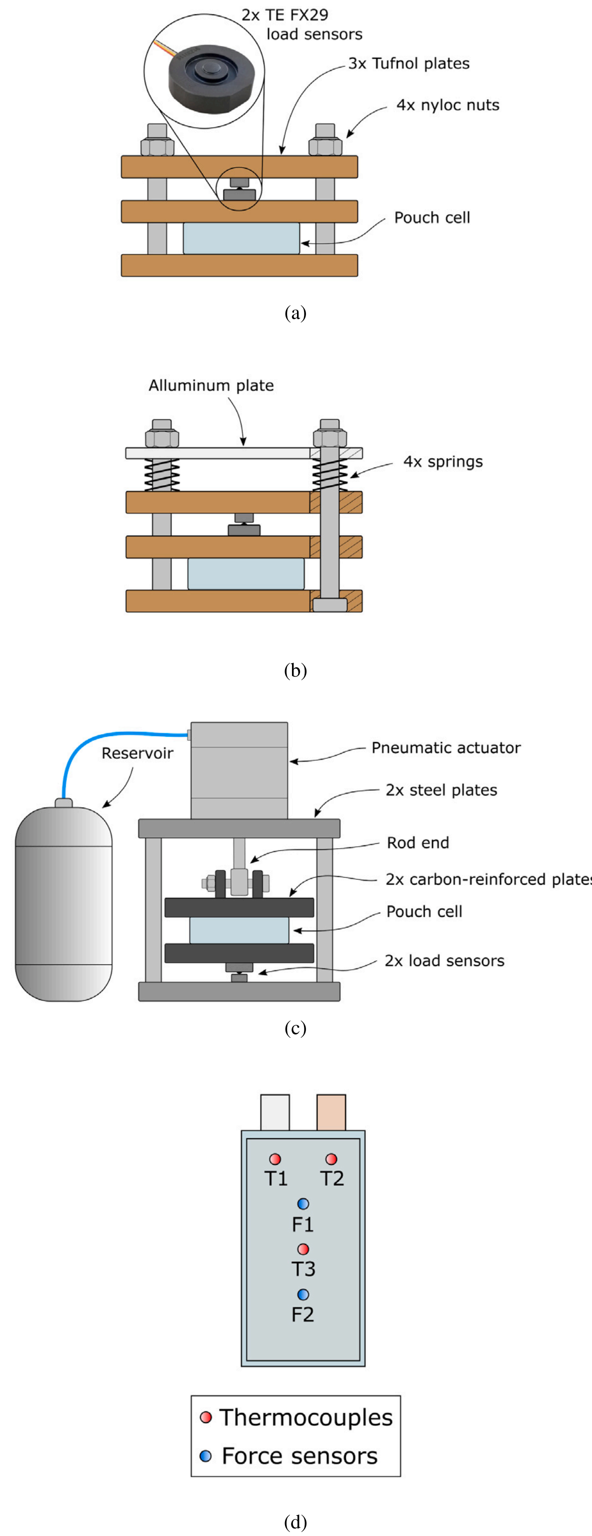

Fig. 2. Front view schematics of the fixtures tested: (a) fixed displacement fixture [12], (b) constant pressure using springs, (c) constant pressure using a pneumatic actuator [6]. (d) Location of the thermocouples and force sensors.

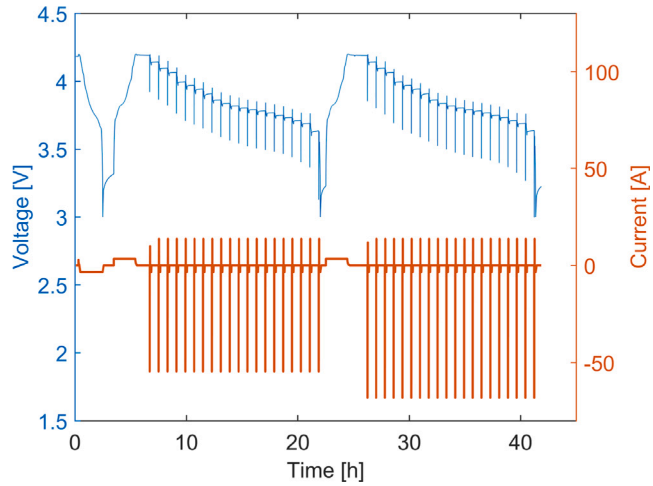

Fig. 3. Dynamic load profile.

The tests were repeated three times on each fixture. To assess the repeatability of the tests, the pressure was completely released and recalibrated to the target pressure before each repetition. This approach ensured that any random or human error would be accounted for in the experiment, providing a more accurate representation of how the devices would be utilized to conduct experiments.

In addition, the fixed displacement device and the constant pressure device using springs were compared using a dummy cell to evaluate the pressure loss due to the stress relaxation of the rig components and bolted connections. The dummy cell was made of solid steel with approximate dimensions to the cell tested.

2.4. Experiment II - Pressure loss during cycling

The second experiment evaluated the pressure loss of the cell during the dynamic load profile shown in Fig. 3. To start the tests from a common reference point, the cell was charged to the maximum cut-off voltage of 4.2 V using a constant current constant voltage (CCCV) charging protocol at C/2. The tests started from 100% SOC to avoid the stack pressure to diverge from the initial calibration due to pressure loss, which would be accentuated if the cell was charged before the tests, for example. Therefore, the stack pressure was calibrated to 90 kPa and the dynamic load profile was run in sequence. The dynamic tests were also conducted at 25 °C.

The dynamic load profile comprises three sections. The first section performs a complete discharge and charge, with a 30-minute rest in between. The second and third sections are HPPC tests [11]. The discharge was performed using constant current (CC) at C/2 to the cut-off voltage of 3 V. The charge was performed by CCCV to 4.2 V, also at C/2. The HPPC tests were composed of 10-s charge and discharge pulses with a 120-s rest period in between. The charge pulse on both HPPC tests were performed at 2C. However, to test the sensitivity of the devices to different C-rates, the first HPPC discharge pulse was set to 8C, and the second to 10C. The charge/discharge pulses were performed at every 5% SOC decrement.

To improve repeatability of the experiments, the load cables and voltage sensing cables setup was not changed throughout the tests [17]. The design of the pressure devices allows swapping cells without disassembling the load and voltage sensing cables [6,12].

3. Results

3.1. Experiment I

Fig. 4 presents the results of the first experiment. The fixed displacement device (a) resulted in the highest pressure loss observed

Table 2
Experiment I results: static pressure loss.

Fixture	Test	P_{loss} [kPa]	P_{loss} [%]	$\bar{x}$ [kPa]	$\sigma_{P_{loss}}$ [kPa]
	1	−15.3	−17	−11.5	
Fixed displacement	2	−7.2	−8.2	−5.2	6.23
	3	−3.1	−3.5	−2.3	
	1	−1	−1.1	−0.77	
Constant pressure (springs)	2	−0.77	−0.9	−0.61	0.14
	3	−0.76	−0.8	−0.62	
	1	−2.25	−2.5	−1.5	
Constant pressure (pneumatic)	2	−1.5	−1.7	−1.1	0.53[a]
	3	−8.6	−9.4	−5.1	

[a] Standard deviation excluding test 3.

among the fixtures tested, decaying as much as 15.3 kPa (17%) in 48 h from the initial 90 kPa. The significant pressure loss was attributed to the stress relaxation of the bolted connections [13,14], although, to a lesser extent, the stress relaxation of the cell due to its viscoelastic properties might also have a contribution [10,16]. Furthermore, the magnitude of the pressure loss was inconsistent among the tests. Even though the pressure monotonically decayed similarly in all tests, the standard deviation of the pressure loss was $\sigma_{P_{loss}}$ = 6.2 kPa, which is significantly higher than the other devices tested. Higher standard deviations indicates lower degree of repeatability of the experiments. More specifically, the fixed displacement device resulted in a standard deviation two orders of magnitude higher than the spring-based device, and one order of magnitude higher than the pneumatic-based device.

In contrast, Fig. 4(b) shows that the constant pressure device using coil springs had the lowest pressure loss among the devices tested, decaying 1 kPa (1.1%) in the worst case (test 1), 0.76 kPa (0.8%) in the best case (test 3). Furthermore, the tests were more consistent, resulting in a standard deviation of the pressure loss of $\sigma_{P_{loss}}$ = 0.14 kPa. Lastly, Fig. 4(c) presents the pressure loss from the tests with the pneumatic device. The first two tests resulted in a pressure loss of 2.25 kPa (2.5%), and 1.5 kPa (1.7%), respectively. However, it significantly increased to 8.6 kPa (9.4%) in the third test, which was likely to be caused by an air leakage in one of the pneumatic connections. Nevertheless, the magnified details in both (b) and (c) reveal that the most significant pressure loss occurs within the initial hour of relaxation, followed by a gradual decaying rate in the subsequent hours. Excluding test 3, the standard deviation of the pressure loss was $\sigma_{P_{loss}}$ = 0.5 kPa.

Fig. 4(d) shows the results of tests performed with the steel dummy cell. Each device was tested three times. The spring-based device is represented by a solid black line, and the fixed displacement device by a dashed blue line. Assuming the stiffness of the dummy cell is several orders of magnitude higher than the actual cell, the results indicate that the rig's stiffness is insufficient to maintain pressure without mitigating stress relaxation in the bolted connections [13,14].

The pressure variation of the data is further explored in the box plot of Fig. 4(e). The upper and lower quartiles represent the 75th and 25th percentiles, respectively, and the dots represent data points exceeding 1.5 times the interquartile range (IQR). The distribution of pressure using the fixed displacement device was higher than the distribution of the data using the constant pressure devices, except for test 3 of the pneumatic actuator, where the air leakage occurred. Table 2 summarizes the results from the tests, where P_{loss} is the pressure loss, $\bar{x}$ is the mean pressure loss, and $\sigma_{P_{loss}}$ is the standard deviation of the pressure loss.

3.2. Experiment II

Fig. 5(a) presents the pressure loss in the first part of the dynamic tests. The pressure build-up happened at a faster rate in the pneumatic device compared to the fixed displacement and spring devices. After the initial increase, the pressure remained approximately constant until the

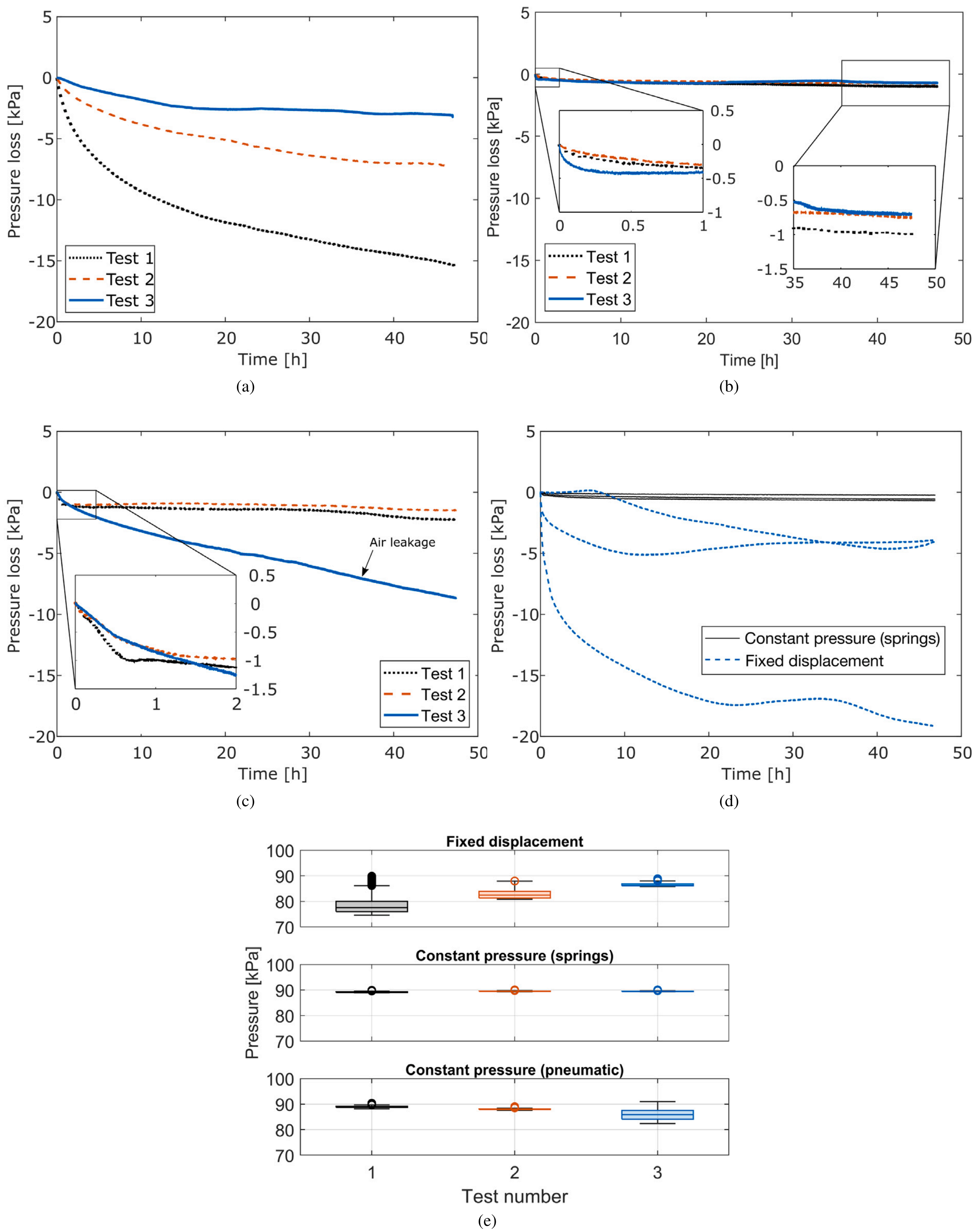

Fig. 4. Experiment I results. Static pressure loss of (a) fixed displacement device, (b) constant pressure device using coil springs, and (c) constant pressure device using pneumatic actuator. (d) Pressure loss of the fixed displacement and spring devices tested with a steel dummy cell (e) Box plot of the pressure distribution during the tests. (For interpretation of the references to colour in this figure legend, the reader is referred to the web version of this article.)

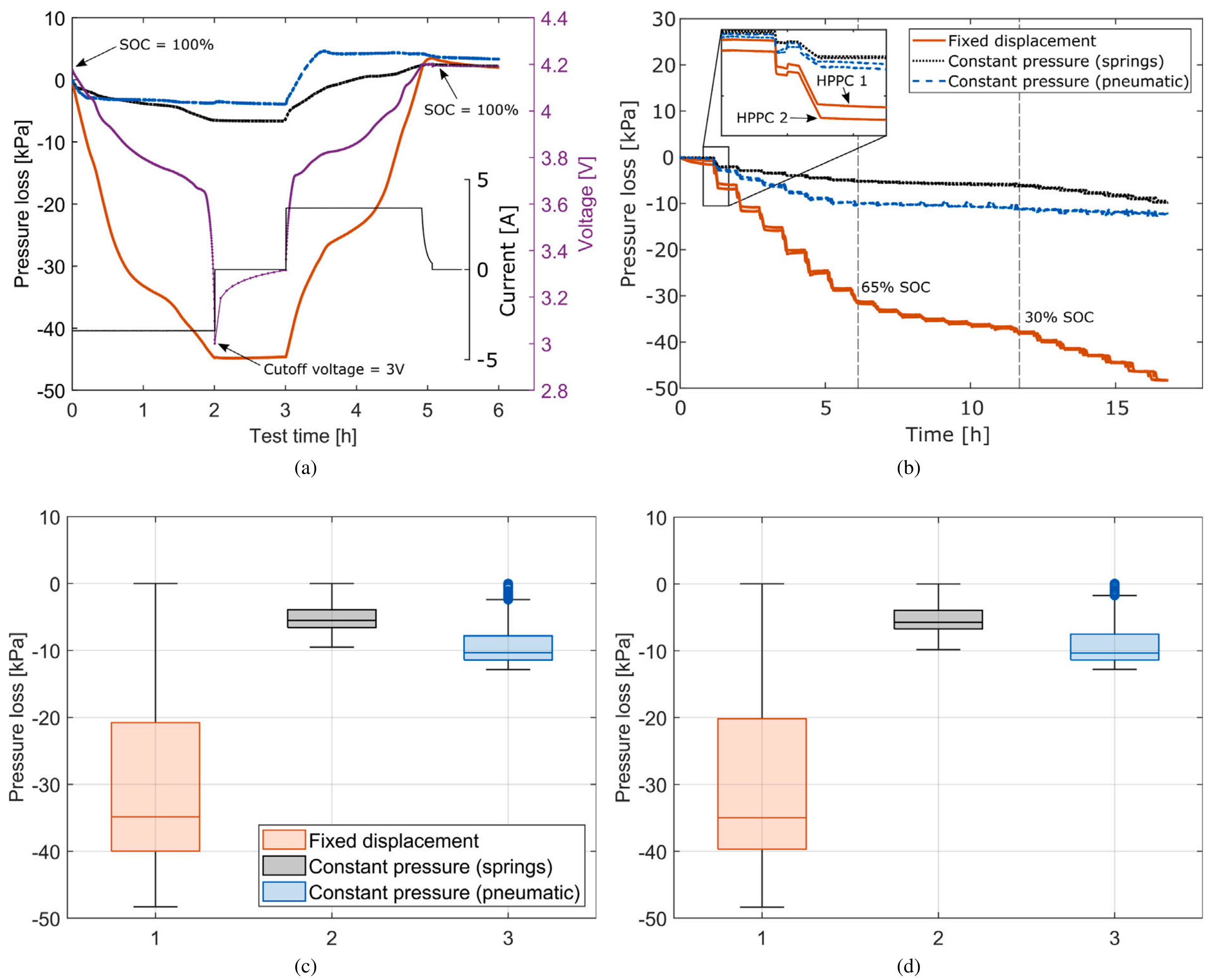

Fig. 5. Experiment II results. (a) C/2 discharge and charge cycle, (b) overlay of the pressure loss from HPPC tests 1 and 2, (c) box plot of the pressure loss from HPPC 1. (d) box plot of the pressure loss from HPPC 2.

Table 3
Experiment II results: HPPC tests.

Fixture	HPPC	P_{loss} [kPa]	P_{loss} [%]	$\bar{x}$ [kPa]	$\sigma_{P_{loss}}$ [kPa]
Fixed displacement	1	−48.3	−50.8	−30.1	0.06
	2	−48.4	−50.8	−29.9	
Constant pressure (springs)	1	−9.5	−10.1	−5.2	0.22
	2	−9.8	−10.4	−5.4	
Constant pressure (pneumatic)	1	−12.9	−13.4	−9.1	0.06
	2	−12.8	−14	−10	

end of the charging section. A closer look reveals that, in the discharge section, the pressure decay of the pneumatic device also happened at a faster rate, remaining constant thereafter. This behaviour suggests the non-linearities of the pneumatic system play a role in how the pressure is released and resisted by the cell. In contrast, the fixed displacement and spring devices appear to follow a profile of pressure change in agreement to what has been reported in the literature [18,19]. The analysis of the maximum and minimum values of the pressure data shows that all devices maintained consistent maximum and minimum pressure values during full charge and discharge cycles. However, when the cell was fully charged to 100% SOC, the pressure exceeded the initial calibration of 90 kPa in all devices. The reasons are not fully understood and need further investigation.

The second and third part of the dynamic tests, HPPC tests 1 and 2, are further explored in Fig. 5(b). The pressure variation during both HPPC tests are overlaid for enhanced visualization. The analysis of each device indicates a similar pressure decay for both tests, even though HPPC 1 employed a discharge rate of 8C and HPPC 2, 10C. However, the magnified detail of the first charge and discharge pulses shows that pressure loss in the fixed displacement device was less consistent compared to the constant pressure devices. The pressure measurement was somewhat shifted due to a higher loss of pressure at the beginning of the second HPPC test. Furthermore, the fixed displacement and spring devices exhibited a pressure variation with similar characteristics. Higher rates of pressure decay were observed in two SOC ranges: from 100% SOC to 65% SOC, and from 30% until 5%. The pneumatic device resulted in a higher rate of pressure loss until 60% SOC, decreasing and stabilizing after until the end of the SOC range.

Fig. 5(c–d) explores the distribution of pressure loss for the HPPC test 1 (d), and for the HPPC test 2 (e). The fixed displacement device resulted in the highest variation of pressure in both tests (−51%). In contrast, the lowest variation was found from the spring device (−10%). Finally, the pressure variation of the pneumatic device was −13% in the first test, and −14% in the second. The box plot reveals that all three devices resulted in consistent pressure variation on both HPPC tests. This is further demonstrated by the small standard deviation of the pressure loss presented in Table 3. However, the repeatability of the devices in the dynamic tests cannot be inferred without further replicates of the tests similarly to the first experiment. Nevertheless, based on the results from the first experiments, it is expected that better repeatability can be achieved using the spring-based device, and

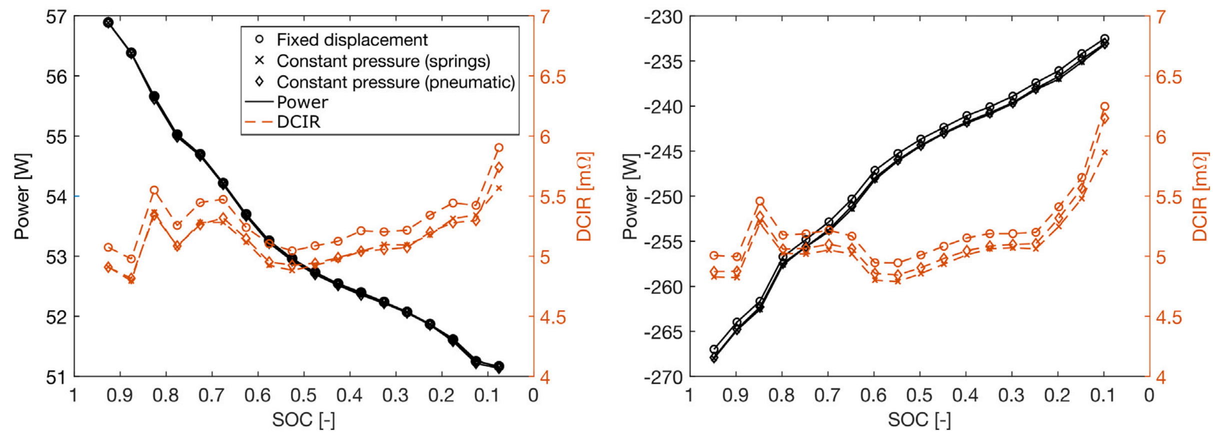

(a) (b)

Fig. 6. Power output and DCIR measurements during the HPPC test (a) 2C charge pulses (b) 10C discharge pulses.

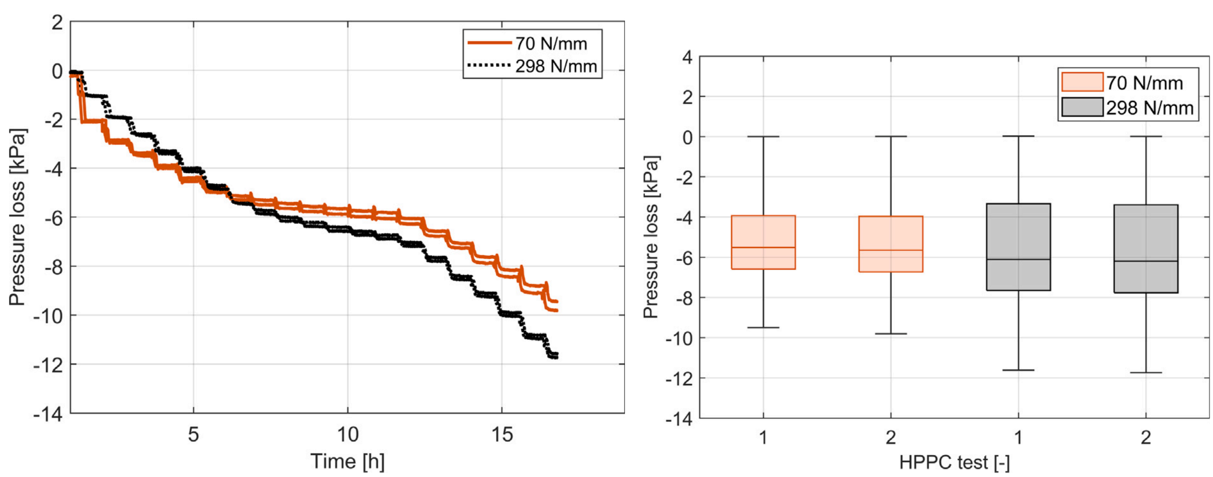

(a) (b)

Fig. 7. Effects of spring stiffness of the spring-based device in the pressure variation. (a) Overlay of the pressure loss of the HPPC tests 1 and 2. (b) Distribution of the pressure loss.

with the pneumatic device as long as the pressure of the system is maintained constant.

For completeness, the power output and the direct current internal resistance (DCIR) of the cell during the HPPC tests are presented in Fig. 6 for the charge pulses (a) and the discharge pulses (b). The DCIR was computed using the voltage drop caused by the constant current pulse. The cell tested demonstrated low sensitivity to stack pressure in both power output and internal resistance, highlighting that the choice of rig can have varying levels of impact depending on whether the cell being tested is sensitive to the levels of stack pressure tested. The power output difference between the devices was negligible for the 2C charge pulses. However, further investigation of the DCIR reveals that the fixed displacement device resulted in a slightly higher internal resistance compared to the constant pressure devices. From the literature, there is an inverse relationship between internal resistance and stack pressure [6]. However, the difference in internal resistance observed was constant across the SOC range, which suggests the DCIR difference observed was likely not a result of the use of a different pressure device. The reason is that all devices were calibrated to the same initial 90 kPa. Additionally, because of the higher pressure loss observed for the fixed displacement device (Fig. 5b), any DCIR deviations due to pressure would be perceived as an increased difference along the SOC range. Furthermore, the measured ambient temperature fluctuations were within the accuracy range of the type-T thermocouples used. Similar results were observed in Fig. 6(b), where the power output difference due to the higher DCIR resistance becomes visible due to the high C rate applied in the pulses. Further investigation would be needed to evaluate the statistical significance of the DCIR differences observed. A comprehensive analysis of the electrical response of pouch cells to external pressure is outside the scope of the current paper, but certainly warrants further research.

To further investigate the effects of the spring stiffness in the pressure variation during the dynamic tests, the 70 N/mm setup was increased to 298 N/mm, an increase of 4.25 times. Even though the increase in the spring rate was significant, Fig. 7(a) demonstrates that the spring-based device is relatively insensitive to the spring stiffness. The pressure variation was expected to be higher in the stiffer setup because, according to the Hooke's law, higher spring stiffness requires less compression for the same preload (initial stack pressure). This means that, as the cell contracts during discharge, the effects of the spring extension are higher for stiffer springs. In other words, it looses more pressure for the same amount of displacement (contraction) of the cell during discharge. However, the relationship between spring stiffness and the pressure variation is not linear because of the viscoelastic properties of the cell. Indeed, the pressure decay observed in Fig. 7(b) was only 21% in the context of a >400% increase in stiffness. Comparing the two setups in the first HPPC test, the pressure loss between the soft and stiff setups were respectively −9.5 and −11.6 kPa. And in the second HPPC test, −9.8 and −11.7 kPa, respectively.

4. Summary and conclusions

This study investigated the impact of stack pressure fixture designs on testing lithium-ion pouch cells. In particular, how well different fixtures concepts apply stack pressure consistently over time. The pressure loss was evaluated from an initial stack pressure of 90 kPa for a cell resting for 48 h. Additionally, dynamic tests were performed by charging and discharging the cell at constant current, and by HPPC tests at high C rates.

Experiments with the fixed displacement device resulted in high variations of stack pressure during cycling, a significant pressure loss during the static test, and a high standard deviation of the experiments. This design failed to mitigate the stress relaxation of the rig, and the high standard deviation of results suggests the experiments were inconsistent.

The best results were achieved with the pneumatic and spring-based constant pressure devices. However, the added mechanical complexity of the pneumatic device and potential air leakages requires careful management. The potential of the pneumatic concept is better explored when paired with active control systems, such as the system developed in [20]. On the other hand, the constant pressure device, using springs, offers a balanced compromise between complexity and pressure control. The pressure change during cycling can be tuned by changing the spring stiffness of the system. This is advantageous for testing cells with large volume expansion, such as cells with composite Si anode [9] or lithium-metal batteries [21] that require careful pressure and volume control. Stiffer spring rates lead to higher pressure variation, whereas soft spring rates attenuate it. However, further research is needed to understand the relationship between the spring rates and the pressure variation of the cell during cycling.

CRediT authorship contribution statement

Adriano Schommer: Writing – review & editing, Writing – original draft, Visualization, Validation, Methodology, Investigation, Formal analysis, Data curation, Conceptualization. **Miguel Orozco Corzo:** Writing – original draft, Visualization, Validation, Investigation. **Paul Henshall:** Writing – review & editing, Validation, Supervision, Investigation. **Denise Morrey:** Supervision, Resources, Project administration. **Gordana Collier:** Supervision, Project administration.

Funding

This research received no external funding.

Declaration of competing interest

The authors declare that they have no known competing financial interests or personal relationships that could have appeared to influence the work reported in this paper.

Acknowledgement

The authors wish to thank the Oxford Brookes University, United Kingdom for financial and technical support.

Data availability

The data used in this paper is available in https://doi.org/10.5281/zenodo.13755167. The engineering drawings of the fixed displacement device developed by Lukow and Planden are available in [12]. The drawings of the pneumatic actuator developed in [6] are available upon request from the authors.

References

[1] G.L. Plett, Battery Management Systems, Volume I: Battery Modeling, Vol. 1, Artech House, 2015.
[2] S. Hahn, S. Theil, J. Kroggel, K.P. Birke, Pressure prediction modeling and validation for lithium-ion pouch cells in buffered module assemblies, J. Energy Storage 40 (2021) 102517.
[3] J. Cannarella, C.B. Arnold, State of health and charge measurements in lithium-ion batteries using mechanical stress, J. Power Sources 269 (2014) 7–14.
[4] L. Aiello, P. Ruchti, S. Vitzthum, F. Coren, Influence of pressure, temperature and discharge rate on the electrical performances of a commercial pouch Li-ion battery, Batteries 10 (3) (2024) 72.
[5] Y.C. Zhang, O. Briat, J.-Y. Deletage, C. Martin, G. Gager, J.-M. Vinassa, Characterization of external pressure effects on lithium-ion pouch cell, in: 2018 IEEE International Conference on Industrial Technology, ICIT, IEEE, 2018, pp. 2055–2059.
[6] A. Leonard, B. Planden, K. Lukow, D. Morrey, Investigation of constant stack pressure on lithium-ion battery performance, J. Energy Storage 72 (2023) 108422.
[7] A.S. Mussa, M. Klett, G. Lindbergh, R. Wreland Lindström, Effects of external pressure on the performance and ageing of single-layer lithium-ion pouch cells, J. Power Sources 385 (2018) 18–26.
[8] A. Barai, Y. Guo, A. McGordon, P. Jennings, A study of the effects of external pressure on the electrical performance of a lithium-ion pouch cell, in: 2013 International Conference on Connected Vehicles and Expo, ICCVE, IEEE, 2013, pp. 295–299.
[9] V. Müller, R.-G. Scurtu, K. Richter, T. Waldmann, M. Memm, M.A. Danzer, M. Wohlfahrt-Mehrens, Effects of mechanical compression on the aging and the expansion behavior of Si/C-composite| NMC811 in different lithium-ion battery cell formats, J. Electrochem. Soc. 166 (15) (2019) A3796–A3805.
[10] J. Cannarella, C.B. Arnold, Stress evolution and capacity fade in constrained lithium-ion pouch cells, J. Power Sources 245 (2014) 745–751.
[11] PNGV Battery Test Manual, Revision 3, Tech. Rep., Idaho National Lab.(INL), Idaho Falls, ID (United States), 2001.
[12] K. Lukow, B. Planden, Modular battery pressure fixture, 2021, URL https://github.com/katielukow/MBPF.
[13] V. Caccese, K.A. Berube, M. Fernandez, J.D. Melo, J.P. Kabche, Influence of stress relaxation on clamp-up force in hybrid composite-to-metal bolted joints, Compos. Struct. 89 (2) (2009) 285–293.
[14] Y. Xie, Y. Xiao, J. Lv, Z. Zhang, Y. Zhou, Y. Xue, Influence of creep on preload relaxation of bolted composite joints: Modeling and numerical simulation, Compos. Struct. 245 (2020) 112332.
[15] B. Rieger, S.V. Erhard, K. Rumpf, A. Jossen, A new method to model the thickness change of a commercial pouch cell during discharge, J. Electrochem. Soc. 163 (8) (2016) A1566.
[16] R. Shen, S. Niu, G. Zhu, K. Wu, H. Zheng, Mechanical behavior analysis of high power commercial lithium-ion batteries, Chin. J. Chem. Eng. 58 (2023) 315–322.
[17] J. Taylor, A. Barai, T. Ashwin, Y. Guo, M. Amor-Segan, J. Marco, An insight into the errors and uncertainty of the lithium-ion battery characterisation experiments, J. Energy Storage 24 (2019) 100761.
[18] X. Cai, C. Zhang, Z. Chen, L. Zhang, D.U. Sauer, W. Li, Characterization and quantification of multi-field coupling in lithium-ion batteries under mechanical constraints, J. Energy Chem. (2024).
[19] B. Rieger, S. Schlueter, S.V. Erhard, J. Schmalz, G. Reinhart, A. Jossen, Multi-scale investigation of thickness changes in a commercial pouch type lithium-ion battery, J. Energy Storage 6 (2016) 213–221.
[20] T. Deich, S.L. Hahn, S. Both, K.P. Birke, A. Bund, Validation of an actively-controlled pneumatic press to simulate automotive module stiffness for mechanically representative lithium-ion cell aging, J. Energy Storage 28 (2020) 101192.
[21] Q. Wang, B. Liu, Y. Shen, J. Wu, Z. Zhao, C. Zhong, W. Hu, Confronting the challenges in lithium anodes for lithium metal batteries, Adv. Sci. 8 (17) (2021) 2101111.